Detection of tumour progression in the follow-up of irradiated low-grade astrocytomas: comparison of 3-[^{123}I]iodo-α-methyl-L-tyrosine and ^{99m}Tc-MIBI SPET

Marcus Henze[1, 2], Ashour Mohammed[1], Heinz Schlemmer[4], Klaus K. Herfarth[5], Walter Mier[1], Michael Eisenhut[3], Jürgen Debus[5], Uwe Haberkorn[1, 2]

[1] Department of Nuclear Medicine, University of Heidelberg, Germany
[2] Clinical Cooperation Unit Nuclear Medicine, German Cancer Research Center, Im Neuenheimer Feld 280, 69120 Heidelberg, Germany
[3] Division Radiochemistry and Radiopharmacology, German Cancer Research Center, Heidelberg, Germany
[4] Division Oncological Diagnostics and Therapy, German Cancer Research Center, Heidelberg, Germany
[5] Division Radiation Oncology, German Cancer Research Center, Heidelberg, Germany

Received 8 April and in revised form 25 May 2002 / Published online: 20 August 2002

Abstract. Conventional MRI often fails to distinguish between progressive tumour and radiation injury, because both appear as mass lesions with unspecific Gd-DTPA enhancement. Furthermore, the sensitivity of FDG PET for the evaluation of malignant lesions in the brain is limited owing to high cortical uptake. The aim of this study was to assess the potential of alternative SPET tracers in the same group of patients. 35.2±20.1 months after stereotactic radiotherapy (59.3±4.2 Gy) of low-grade astrocytomas (median WHO II), 16 patients, presenting 25 Gd-DTPA-enhancing lesions on MRI, were examined by SPET. Lesions were classified as progressive tumour (PT, *n*=17) or non-PT (nPT, *n*=8) based on prospective follow-up (clinical examination, MRI, proton-MR spectroscopy) for 25.6±6.7 months after SPET. SPET scans were performed 15 and 60 min after injection of 694±67 MBq hexakis(2-methoxyisobutylisonitrile)^{99m}Tc(I) (MIBI). 3-[^{123}I]iodo-α-methyl-L-tyrosine (IMT) SPET was acquired 15 min after injection of 291±58 MBq IMT. Lesion-to-normal tissue ratios (l/n) for IMT (l/n_{IMT}) and MIBI (l/n_{MIBI}) were calculated using a reference region mirrored to the contralateral hemisphere. Using IMT, significantly higher ratios (P<0.001) were found in PT (1.7±0.4) than in nPT (1.1±0.1). For MIBI, there was no statistically significant difference (P=0.206) between PT (3.7±2.8) and nPT (1.8±1.8). Sensitivities for MIBI and IMT were 53% and 94%, and specificities 75% and 100%, respectively. Positive predictive values for MIBI and IMT respectively reached 80% and 100%, and negative predictive values were 46% and 90%. In conclusion, in contrast to MIBI, IMT showed almost no overlap between the PT and the nPT group. The sensitivity, specificity and predictive values of IMT SPET were obviously higher than those of MIBI SPET. IMT is considered to be a useful tracer for differentiating PT from nPT in the follow-up of irradiated low-grade astrocytomas.

Keywords: ^{123}I-IMT – ^{99m}Tc-MIBI – Low-grade astrocytoma – Radiotherapy

Eur J Nucl Med (2002) 29:1455–1461
DOI 10.1007/s00259-002-0896-0

Marcus Henze (✉)
Department of Nuclear Medicine,
University of Heidelberg, Germany
e-mail: m.henze@dkfz.de
Tel.: +49-6221-422477, Fax: +49-6221-422510

Introduction

In the 15- to 34-year age group, brain tumours are the third most common cause of death due to cancer. In persons older than 20 years, gliomas account for more than 90% of primary intracranial tumours. About 25% of all gliomas are low-grade astrocytomas (LGAs) [1]. The majority of LGAs are not amenable to complete resection. Radiotherapy is the most effective non-surgical therapy, with a low risk of inducing radiation necrosis when conventional techniques are used [2, 3]. Radiation necrosis is a much more common consequence of more aggressive, and now widely used, treatment protocols that deliver high local doses to small volumes (e.g. stereotactic radiotherapy or brachytherapy) [4]. However, necrosis is mainly confined to white matter and remains an idiosyncratic phenomenon that cannot be predicted. In recurrent LGA, malignant progression to a high-grade tumour with a median survival of only 10 months is very common, occurring in about two-thirds of the patients

[5]. This necessitates early detection and intervention in cases of tumour progression, as new treatment approaches improve local control and patient survival.

The differentiation between tumour recurrence/progression and radiation injury/necrosis is one of the most difficult tasks in oncological neuroradiology. Anatomical distortion and scarring after therapy often impairs detection of residual or recurrent disease [6, 7]. In addition to clinical findings, contrast-enhanced magnetic resonance imaging (MRI) is currently used to measure therapy response. Single conventional MRI scans often fail to distinguish recurrent tumour from radiation injury or necrosis, because both cause disturbances of the blood-brain barrier (BBB), leading to unspecific contrast media enhancement. Moreover, corticosteroids have a profound effect on the degree of Gd-DTPA enhancement, on the peritumoural oedema and on the volume of enhancement [8]. Even the biopsy of an oedematous or gliotic site is often non-diagnostic, because both viable and necrotic cells are found in tissue specimens.

An accurate indicator of tumour metabolism and vitality is pivotal to the evaluation of the treatment in order to avoid long-term follow-up and loss of time. Many authors have reported that by measuring glucose metabolism, 2-[^{18}F]fluoro-2-deoxyglucose (FDG) positron emission tomography (PET) is able to differentiate radiation necrosis from recurrent tumour [9, 10, 11, 12]. However, FDG-PET has the drawbacks of high cost and limited sensitivity in detecting low-grade tumours due to the high glucose consumption of the normal cortex and basal ganglia. Labelled amino acids may overcome this problem because of their low uptake in normal brain [13]. Furthermore, they play a minor role in the metabolism of inflammatory cells, resulting in a higher specificity as compared with FDG [14]. Numerous studies support the application of the SPET tracers 3-[^{123}I]iodo-α-methyl-L-tyrosine (IMT) and hexakis(2-methoxyisobutylisonitrile)^{99m}Tc(I) (MIBI) in untreated primary brain tumours, but very few have investigated their use in patients with previously irradiated brain tumours; furthermore, when they have done so, most of the tumours have been of higher grade. Transmembrane transport via the L-carrier system for large neutral amino acids is thought to be the main determinant of the IMT uptake in brain tumours [15]. IMT is not incorporated into proteins, and after rapid uptake it reaches a plateau within 5 min after injection and remains stable for at least 1 h before being slowly washed out [16]. Studies directly comparing the diagnostic utility of different tracers for this clinically important task have been recommended [17]. However, it still remains unclear which tracer gives more accurate information on tumour progression or recurrence. Accordingly, this prospective study evaluated the SPET tracers IMT and MIBI in the same patient group to determine whether they allow the identification of progressive tumour in previously irradiated LGAs.

Materials and methods

Patients. We examined 16 patients (10 male, 6 female, mean age 42.9±9.7 years, Table 1) initially suffering from histologically proven LGAs (median WHO grade II). Patients were treated by stereotactic radiotherapy (59.3±4.2 Gy). All patients gave their informed consent prior to their inclusion. The study was approved by the local ethical committee.

On average 35.2±20.1 months after radiotherapy, the patients presented new Gd-DTPA-enhancing lesions (n=25) on MRI, which did not allow differentiation between progressive tumour (PT) and non-PT (nPT) at this point in time. MRI was closely followed by SPET scans, as described below. Lesions were classified

Table 1. Patient data

Patient no.	Gender	Age (yr)	Radiation dose (Gy)	Period between radiotherapy and SPET (mo)	Follow-up period after
1	f	51	58	39	18
2	m	54	56	26	28
3	m	29	60	17	22
4	m	41	58	12	20
5	m	34	66	60	28
6	m	44	60	42	23
7	m	69	64	56	20
8	m	33	56	8	28
9	f	48	63	27	32
10	m	39	54	22	19
11	f	37	52	31	33
12	f	43	61	61	15
13	f	47	64	74	31
14	m	39	58	51	29
15	m	36	64	20	40
16	f	43	54	17	23

f, Female; m, male

as PT or nPT based on prospective follow-up (clinical examination, MRI, proton-MR spectroscopy) for 25.6±6.7 months after SPET. The classification was not influenced by the results of the SPET studies. MRI including multiplanar T1-weighted and T2-weighted spin-echo imaging followed by multiplanar Gd-DTPA-enhanced T1-weighted imaging was repeated every 3–6 months using a 1.5-T MR scanner (Siemens AG, Erlangen, Germany). Intervals were shortened in the case of worsening of symptoms. Because repeated proton-MR spectroscopy was shown to improve the differentiation between treatment-induced necrosis and residual or recurrent brain tumour, it was included in the MRI protocol in doubtful cases [18, 19, 20].

In the *PT group* (17 lesions), patients received 59.3±4.1 Gy. The interval between radiotherapy and SPET was 37.8±21.4 months and lesions were followed up for an additional 24.5±5.7 months after SPET until final classification was made. The patients in the *nPT group* (eight lesions) received 58.3±5.7 Gy. In this group, the interval between radiotherapy and SPET was 23.6±15.5 months and the follow-up was 30.9±7.2 months after SPET.

MIBI SPET. MIBI (Sestamibi, DuPont Pharma S.A., Brussels, Belgium) was prepared according to the manufacturer's instructions. SPET scans were started 15 and 60 min after intravenous injection of 694±67 MBq MIBI. Quality control was carried out according to the manufacturer's instructions. SPET was obtained using a dual-head gamma camera (Siemens MULTISPECT 2) equipped with high-resolution collimators. Sixty-four projections were obtained over 360°. The radius of rotation was individually minimised, being limited by the patient's shoulders. Data were registered for 40 s in each projection and were recorded in a 64×64 matrix. The zoom factor was 1.78. Images were reconstructed by filtered back-projection using a Butterworth filter (f_C=0.5 Nyquist, order=8). Attenuation correction (first-order, 0.12/cm) was performed using the post-reconstruction method of Chang [21].

IMT SPET. Patients fasted overnight before tracer injection. In order to prevent possible uptake of free iodine, the thyroid gland was blocked with sodium perchlorate. IMT was essentially prepared as described previously [22]. The physical purity of ^{123}I (Forschungszentrum Karlsruhe, Germany) was ≥99.65%. In short, radioiodination of α-methyl-L-tyrosine was performed using the KIO_3/[^{123}I]iodide method: 20 µl of a 10 m*M* (in 1 *N* HCl) solution of α-methyl-L-tyrosine (Sigma-Aldrich) was mixed with 5 µl of 50 m*M* KIO_3 (H_2O) and 400–1,200 MBq [^{123}I]iodide. After 10 min, the mixture was purified with an RP18-HPLC column using a gradient of methanol (0%–100% in 30 min) at a flow rate of 0.7 ml/min. The aqueous phase consisted of 0.9% TRIS buffer (pH 2.6). Under these conditions the ^{123}I-labelled α-methyl-L-tyrosine eluted after 18.2 min. The collected eluate was evaporated to dryness, redissolved in 2 ml sterile 0.9% NaCl solution, neutralized and sterile-filtered. The average radiochemical yield was 95%. Specific activities obtained were 300 GBq/µmol.

IMT accumulates in brain and tumour tissue, reaching a maximum after 15 min, with a washout of 20%–45% at 60 min post injection [23, 24]. Therefore, we started imaging 10 min after intravenous injection of 291±58 MBq IMT. The same gamma camera system (Siemens MULTISPECT 2) as in the sestamibi examination, equipped with medium-energy collimators, was used. The presence of 2.5% high-energy photons in ^{123}I-labelled radiotracers causes image deterioration due to increased scatter and septal penetration. Besides the 159-keV photons, even high-purity ^{123}I emits high-energy photons: 2.4% between 440 and 625 keV and 0.15% between 625 and 784 keV. Thus Dobbeleir et al. recommended the use of medium-energy collimators when semiquantitative image analysis is used [25]. Sixty-four 40-s projections were acquired over 360° using a 64×64 matrix. The radius of rotation was individually minimised, being limited by the patient's shoulders. A zoom factor of 1.78 was chosen. Images were reconstructed by filtered back-projection using a Butterworth filter (f_C=0.5 Nyquist, order=8). First-order attenuation correction (0.12/cm) was performed, using Chang's method [21].

Data analysis. The images were analysed by calculating lesion to normal tissue ratios (l/n). Areas of abnormal tracer uptake were defined as focally increased uptake or as asymmetry in uptake in comparison with the contralateral side. Uptake ratios were calculated using reference regions in the contralateral hemisphere, because of the limitations of obtaining absolute quantification with SPET. Regions of interest (ROIs) were manually delineated on the two transaxial slices with the highest tracer uptake in the lesion. ROIs were placed over the lesions to include all pixels having at least 70% of the maximum uptake of the lesion. Some patients showed no elevated tracer uptake by the Gd-DTPA-enhancing lesion. In these patients the ROI placement was selected with reference to MRI scans. The number of average counts in each ROI was determined for each SPET image. Semiquantitative measurement of tracer uptake was obtained by calculating l/n ratios (l/n_{IMT} and l/n_{MIBI}) for all Gd-DTPA-enhancing lesions using a reference region mirrored to the contralateral hemisphere. Although the possibility that the contralateral hemisphere might exhibit reduced metabolism due to interruption of association fibres between hemispheres cannot be entirely excluded, it has been shown that this effect is negligible [26].

For statistical analysis the SigmaStat V2.0 software (Jandel Corporation San Rafael, Calif., USA) was used. Data were tested for normality using the Kolmogorov-Smirnov test and for equal variance using the Levene Median test. The Mann-Whitney rank sum test was chosen for comparison between the PT and the nPT group, because it has proven to be reliable in populations when both assumptions for the unpaired *t* test are not met. Correlation was calculated using the Spearman rank order test. The $P<0.05$ level was considered statistically significant.

Results were classified as true positive (TP) or false positive (FP), and negative imaging results as true negative (TN) or false negative (FN) for PT. Calculations of sensitivities, specificities and predictive values were based on a cut-off value of l/n=1.3, which allowed the best separation between patient groups for each of the tracers studied. Sensitivity was calculated as #TP/(#TP+#FN), specificity as #TN/(#TN+#FP), positive predictive value (PPV) as #TP/(#TP+#FP) and negative predictive value (NPV) as #TN/(#TN+#FN).

Results

MIBI SPET

For the whole population of patients the ratios ranged between 1.0 and 8.6 (mean 3.0±2.6) for the early scan, and between 1.0 and 7.7 (mean 3.0±2.6) for the delayed scan. The paired *t* test failed to identify a significant difference in l/n ratios between early and delayed SPET

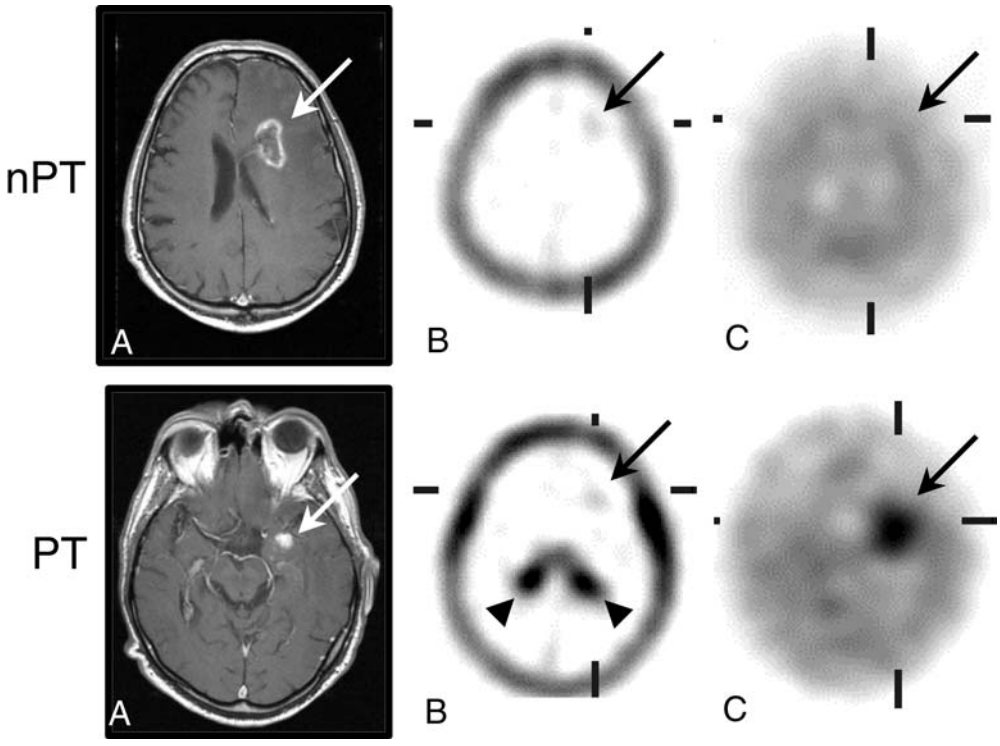

Fig. 1A–C. Example of a male patient with an LGA, which was stereotactically irradiated (64 Gy) 56 months before SPET. He presented two contrast media-enhancing mass lesions on MRI follow-up (**A**). *Upper row:* Radiation necrosis (confirmed by biopsy and clinical and MRI follow-up, *arrows*): false positive MIBI uptake (**B**). Correctly classified as nPT by IMT (**C**). *Lower row:* Progressive tumour (confirmed by clinical and MRI follow-up, *arrows*): correctly classified as PT by MIBI (**B**; normal uptake of the choroid plexus, *arrowheads*) and IMT (**C**)

Table 2. Semiquantitative l/n ratios (mean±SD) for IMT and MIBI

	IMT SPET	MIBI SPET
PT group: l/n (mean±SD)	1.7±0.4	3.7±2.8
nPT group: l/n (mean±SD)	1.1±0.1	1.8±1.8
P	<0.001	0.206

(*P*=0.63). A close correlation existed between early and late MIBI scans (*r*=0.98; *P*<0.001), which indicated that no relevant tracer washout had occurred.

In the nPT group, l/n ratios varied from 1.0 to 7.0 with a mean of 1.8 (±1.8 SD) (Table 2). Twenty-five percent of the non-progressive lesions showed a false positive MIBI uptake (an example is shown in Fig. 1). L/n ratios in the PT group ranged between 1.0 and 8.6 with a mean of 3.7 (±2.8 SD) (Table 2). Forty-seven percent of PTs did not show increased MIBI uptake. There was no statistically significant difference (*P*=0.206) between the PT and the nPT group (Table 2). For the detection of PTs with MIBI, sensitivity was 53%, specificity 75%, NPV 46% and PPV 80% (Figs. 2, 3).

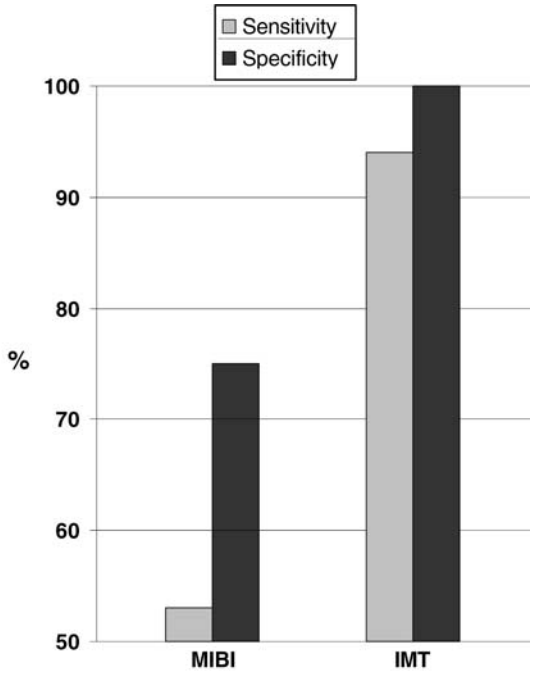

Fig. 2. Sensitivity and specificity for MIBI and IMT

^{123}I-IMT SPET

In the PT group, only a single lesion located in the brainstem did not show increased IMT uptake and, therefore, was classified as false negative. L/n ratios in the PT group ranged between 1.2 and 2.8 with a mean of 1.7 (±0.4 SD) (Table 2). In the nPT group no lesion showed a false positive accumulation of IMT. The l/n ratios in this group varied from 1.0 to 1.3 with a mean of 1.1 (±0.1 SD). Significantly higher ratios were found in the PT group than in the nPT group (*P*<0.001) (Table 2). For the detection of PT, sensitivity was 94%, specificity 100%, NPV 90% and PPV 100% (Figs. 2, 3).

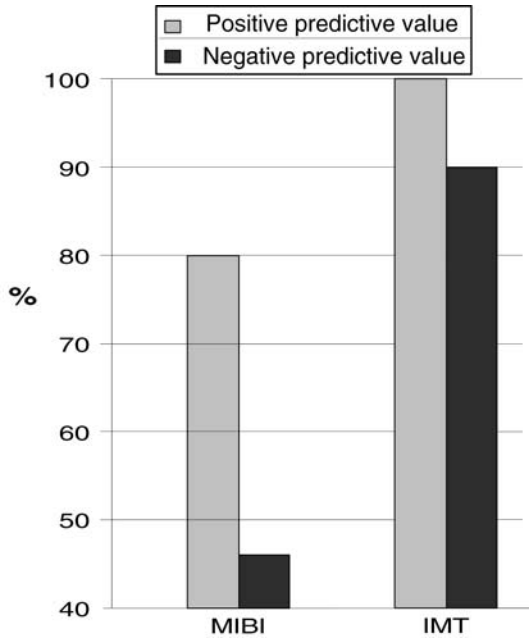

Fig. 3. Predictive values for MIBI and IMT

Discussion

Our multitracer studies in patients with irradiated LGAs indicate that IMT SPET has a high sensitivity (94%) and specificity (100%) for the detection of PT, while MIBI appears to be less sensitive (53%) and specific (75%). In contrast to IMT, MIBI did not allow exclusion of PT owing to its high rate of false negative results.

Although a comparison of different tracers for this clinically relevant task has been proposed [17], no study applying IMT and MIBI in the same population has been published so far. Furthermore, studies using one of these tracers have included only small numbers of irradiated low-grade tumours.

Promising results were reported when MIBI was applied in pretreated high-grade gliomas, [27], whereas studies examining miscellaneous tumour grades showed sensitivities for detection of tumour relapse of between 73% and 88%. Specificities were 85%–91%, PPV 91%–98% and NPV 60%–63% [28, 29]. However, the study reporting the highest values included only a small percentage (27%) of low-grade tumours [28]. In contrast, the lowest sensitivities and specificities were observed in the study with the highest percentage (50%) of low-grade gliomas, making it impossible to exclude tumour recurrence in these patients [29]. In six previously irradiated gliomas, solely of low grade, it was not possible to differentiate with MIBI between tumour and three radiation necroses [30]. MIBI uptake is determined by vascular supply, by the permeability of the BBB and by the density and viability of the tumour cells [31]. Furthermore, a passive influx of MIBI due to the negative potential of the plasma membrane and the mitochondrial inner membrane has been demonstrated [32]. Staudenherz et al. were able to visualise 15 of 25 recurrent high-grade brain tumours with both MIBI and ^{99m}Tc-pertechnetate (PTT). In the remaining ten patients, the tumour was not detected with either of the tracers. They concluded that retention of MIBI reflects no more than damage to the BBB [33]. Within 5 years after initial diagnosis, at least 50% of LGAs undergo malignant transformation and develop a BBB disruption [34]. However, BBB disruption also occurs in radiation necrosis. Accordingly, Gd-DTPA enhancement on MRI indicated damage of the BBB in all our patients as a prerequisite for MIBI uptake.

We also found limited detectability of paraventricular lesions, in accordance with previous reports [31, 35]. This was explained by the distribution pattern of MIBI, as in normal controls uptake is observed in the choroid plexus, the pituitary gland and the scalp [31].

In contrast to the initial MIBI uptake, MIBI washout in delayed imaging (1–4 h p.i.) was related to the expression of the multidrug resistance pump P-glycoprotein (Pgp) [36, 37]. Early imaging as performed in our study offers the highest diagnostic yield and is not affected by the multidrug resistant phenotype [38]. We have no evidence that efflux contributed to the high rate of false negative MIBI scans, since MIBI washout did not occur between early and late SPET scans.

Furthermore, the low tumour detection rate of MIBI as compared with IMT could not be explained by technical factors, given that the same camera system and acquisition parameters were used for both SPET tracers, with the exception of the collimators.

Using IMT, reliable distinction between PT and nPT was possible among our patients, and in particular there were no false positive results. Since IMT competes with structurally related naturally occurring L-amino acids for transport into brain and tumour, which could result in a decrease in sensitivity [15], we examined all patients under fasting conditions. With this procedure, only a single PT lesion located in the brainstem did not show significantly increased IMT uptake (l/n=1.2) and, therefore, was classified as false negative. Unfortunately, at present no commercial kit is available for the preparation of IMT.

In contrast to ^{11}C-tyrosine uptake, IMT uptake reflects amino acid transport rather than the protein synthesis rate, because it is not incorporated into proteins. Protein synthesis and amino acid transport are both accelerated in high- as well as low-grade tumour tissue. In addition to transmembrane tumour uptake, the L-carrier system for large neutral amino acids mediates the transport across the intact BBB [15, 39]. Because IMT is not metabolised, it is washed out of the brain after reaching a maximum uptake at 15 min p.i. [24, 39, 40]. However, IMT has been shown to be a promising tool for evaluation of the biological activity and delineation of the intracerebral infiltration of gliomas [24, 41, 42].

Most studies using IMT in the follow-up after treatment of brain tumours include only a limited number ($n \leq 5$) of low-grade tumours [43, 44]. In one of the largest series, the cerebral uptake of IMT was determined in 27 patients, including nine with low-grade tumours, of whom three underwent radiotherapy. The overall sensitivity for detection of recurrences was 78%, and the specificity 100% [17]. In another study, the sensitivity of IMT for confirmation of low-grade recurrences ($n=8$) proved to be superior to that of FDG [13].

Although cases of a high [^{11}C]methyl-L-methionine uptake in brain abscess [45] and radionecrosis [46] have been described, we observed no false positive results with IMT in our patients. Labelled amino acids play a minor role in the metabolism of macrophages and other inflammatory cells, resulting in a higher specificity as compared with FDG [14]. Therefore, they were presumed to be more suitable for monitoring response to radio- or chemotherapy [47, 48].

As in most other studies, the classification of our patients relies on clinical follow-up and not on biopsy. Particularly after irradiation, gliomas are not homogeneous. Even stereotactically guided biopsy is often inaccurate, because samples may be taken from scarred or gliotic areas and do not necessarily represent total tumour viability [49, 50]. Furthermore, the presence of morphologically intact tumour cells does not indicate recurrence or progression, since these cells may be unable to proliferate after therapy [51]. In our series of patients, lesions were classified based on prospective clinical follow-up including serial MRI and proton-MR spectroscopy for, on average, 25.6 months. This procedure seems to be more reliable as compared to studies using CT and follow-up periods of 6 months [27, 28, 29].

Conclusion

While the results obtained with MIBI SPET in the diagnosis of primary and recurrent high-grade astrocytomas have been encouraging, it appears of less value in the follow-up of LGAs. In spite of the excellent physical properties of MIBI, only IMT allowed reliable differentiation between tumour progression and radiation-related tissue alterations in such cases. Imaging of the amino acid transport with IMT SPET is a valuable additional tool in the follow-up of irradiated LGAs. Its inclusion in the follow-up scheme would allow early non-invasive differentiation of brain lesions exhibiting an ambiguous morphology after radiotherapy. Metabolic imaging using IMT might help to avoid a loss of time due to repeated MRI scans. In cases of tumour progression, this would facilitate earlier initiation of adequate further treatment.

Acknowledgements. The authors would like to thank H. Adam and S. Biedenstein for kind technical assistance in this study.

References

1. Landis SH, Murray T, Bolden S, Wingo PA. Cancer Statistics. *CA Cancer J Clin* 1999; 49:8–31.
2. Herfarth KK, Gutwein S, Debus J. Postoperative radiotherapy of astrocytomas. *Semin Surg Oncol* 2001; 20:13–23.
3. Vick NA, Coroc IS, Eller TW. Reoperation for malignant astrocytoma. *Neurology* 1989; 39:430–432.
4. Li A, Shea WM, Wyn W. Radiosurgery as a part of the initial management of patients with malignant glioma. *J Clin Oncol* 1992; 10:1379–1385.
5. Forsyth PA, Kelly PJ, Cascino TL, Scheithauer BW, Shaw EG, Dinapoli RP, Atkinson EJ. Radiation necrosis or glioma recurrence: is computer-assisted stereotactic biopsy useful? *J Neurosurg* 1995; 82:436–444.
6. Byrne TN. Imaging of gliomas. *Semin Oncol* 1994; 21:162–171.
7. Leeds NE, Jackson EF. Current imaging techniques for the evaluation of brain neoplasms. *Curr Opin Oncol* 1994; 6: 254–261.
8. Davis WK, Boyko OB, Hoffman JM et al. 18-F-FDG PET correlation of gadolinium-enhanced MR imaging of central nervous system neoplasia. *AJNR Am J Neuroradiol* 1993; 14:515–523.
9. Patronas NJ, Di Chiro G, Brooks RA. Work in progress: [^{18}F]Fluordeoxyglucose and positron emission tomography in the evaluation of radiation necrosis of the brain. *Radiology* 1982; 144:885–889.
10. Glantz MJ, Hoffman JM, Coleman RE. The role of F18 FDG PET imaging in predicting early recurrence of primary brain tumors. *Ann Neurol* 1991; 29:347–355.
11. Di Chiro G, Oldfield E, Wright DC, De Michele D, Katz DA, Patronas NJ, Doppman JL, Larson SM, Ito M, Kufta CV. Cerebral necrosis after radiotherapy and/or intraarterial chemotherapy for brain tumors: PET and neuropathologic studies. *AJR Am J Radiol* 1988; 150:189–197.
12. Ishikawa M, Kikuchi H, Miyatake S, et al. Glucose consumption in recurrent gliomas. *Neurosurgery* 1993; 33:28–33.
13. Bader JB, Samnick S, Moringale JR, et al. Evaluation of L-3-[^{123}I]iodo-methyltyrosine SPET and [^{18}F]fluorodeoxyglucose PET in the detection and grading of recurrences in patients pretreated for gliomas at follow-up: a comparative study with stereotactic biopsy. *Eur J Nucl Med* 1999; 26:144–151.
14. Kubota R, Kubota K, Yamada S, et al. Methionine uptake by tumor tissue: a microautoradiographic comparison with FDG. *J Nucl Med* 1995; 36:484–492.
15. Langen KJ, Roosen N, Coenen H, et al. Brain and brain tumor uptake of L-3-[123-I] iodo-methyl tyrosine: competition with natural L-amino acids. *J Nucl Med* 1991; 32:1225–1228.
16. Jager PL, Groen HJM, van der Leest A, van Putten JWG, Pieterman RM, de Vries EGE, Piers DA. L-3-[^{125}I]iodo-alpha-methyl-tyrosine SPECT in non-small cell lung cancer: preliminary observations. *J Nucl Med* 2001; 42:579–585.
17. Kuwert T, Woesler B, Morgenroth C, et al. Diagnosis of recurrent glioma with SPECT and iodine-123-alpha-methyl tyrosine. *J Nucl Med* 1998; 39:23–27.
18. Schlemmer HP, Bachert P, Herfarth KK, Zuna I, Debus J, van Kaick G. Proton MR spectroscopic evaluation of suspicious brain lesions after stereotactic radiotherapy. *AJNR Am J Neuroradiol* 2001; 22:1316–1324.
19. Nelson SJ, Vigneron DB, Dillon WP. Serial evaluation of patients with brain tumors using volume MRI and 3D ^{1}H-MRSI. *NMR Biomed* 1999; 12:123–138.

20. Graves EE, Nelson SJ, Vigneron DB, et al. Serial proton MR spectroscopic imaging of recurrent malignant gliomas after gamma knife radiosurgery. *AJNR Am J Neuroradiol* 2001; 22:613–624.
21. Chang LT. A method for attenuation correction in radionuclide computed tomography. *IEEE Trans Nucl Sci* 1978; 25:638–643.
22. Bubeck B, Eisenhut M, Heimke U, zum Winkel K. Melanoma affine radiopharmaceuticals. I. A comparative study of 131I-labelled quinoline and tyrosine derivatives. *Eur J Nucl Med* 1981; 6:227–233.
23. Langen KJ, Coenen HH, Roosen N, et al. SPECT studies of brain tumors with L-3-[^{123}I] iodo-alpha-methyl tyrosine: comparison with PET, ^{124}IMT and first clinical results. *J Nucl Med* 1990; 31:281–286.
24. Langen KJ, Ziemons K, Kiwit JC, et al.: 3-[^{123}I]iodo-alpha-methyltyrosine and [methyl-^{11}C]-L-methionine uptake in cerebral gliomas: a comparative study using SPECT and PET. *J Nucl Med* 1997; 38:517–522.
25. Dobbeleir AA, Hambye AS, Franken PR. Influence of high-energy photons on the spectrum of iodine-123 with low- and medium-energy collimators: consequences for imaging with ^{123}I-labelled compounds in clinical practice. *Eur J Nucl Med* 1999; 26:655–658.
26. Andrews RJ. Transhemispheric diaschisis: a review and comment. *Stroke* 1991; 22:943–949.
27. Soler C, Beauchesne P, Maatougui K, Schmitt T, Barral FG, Michel D, Dubois F, Brunon J. Technetium-99m sestamibi brain single-photon emission tomography for detection of recurrent gliomas after radiation therapy. *Eur J Nucl Med* 1998; 25:1649–1657.
28. Maffioli L, Gasparini M, Chiti A, et al. Clinical role of technetium-99m sestamibi single-photon emission tomography in evaluating pretreated patients with brain tumours. *Eur J Nucl Med* 1996; 23:308–311.
29. Lamy-Lhullier C, Dubois F, Blond S et al. Importance of cerebral tomoscintigraphy using Tc-labelled sestamibi in the differential diagnosis of recurrent tumor vs. radiation necrosis in subtentorial glial tumors in the adult. *Neurochirurgie* 1999; 45:110–117.
30. Baillet G. Albuquerque L, Chen Q, Poisson M, Delattre JY. Evaluation of single-photon emission tomography imaging of supratentorial brain gliomas with technetium-99m-sestamibi. *Eur J Nucl Med* 1994; 21:1061–1066.
31. Bagni B, Pinna L, Tamarozzi R, Cattaruzzi E, Marzola MC, Bagni I, Ceruti S, Valentini A, Zanasi A, Mavilla L, Guerra PU, Merli AG. SPET imaging of intracranial tumours with ^{99m}Tc-sestamibi. *Nucl Med Commun* 1995; 16:258–264.
32. Piwnica-Worms D, Kronauge JF, Chiu ML. Uptake and retention of hexakis (2methoxy isobutyl isonitrile) technetium (I) in cultured chick myocardial cells: mitochondrial and plasma membrane potential dependence. *Circulation* 1990; 82:1826–1838.
33. Staudenherz A, Fazeny B, Marosi C, et al. Does ^{99m}Tc-sestamibi in high-grade malignant brain tumors reflect blood-brain barrier damage only?. *Neuroimage* 2000; 12:109–111.
34. McCormack BM, Miller DC, Budzilovic GN, Voorhees GJ, Ransohoff J. Treatment and survival of low-grade astrocytoma in adults: 1977 – 1988. *Neurosurgery* 1992; 31:636–642.
35. Macapinlac A, Scott A, Cluser C, et al. Comparison of Tl-201 and Tc-99m MIBI with MRI in the evaluation of recurrent brain tumors. *J Nucl Med* 1992; 33:867.
36. Piwnica-Worms D, Chiu ML, Budding M, et al. Functional imaging of multidrug-resistant P-glycoprotein with an organotechnetium complex. *Cancer Res* 1993; 53:977–984.
37. Taki J, Sumiya H, Asada N, et al. Assessment of P-glycoprotein in patients with malignant bone and soft tissue tumors using technetium-99m-MIBI scintigraphy. *J Nucl Med* 1998; 39:1179–1184.
38. Leitha T, Glaser G, Lang S. Is early sestamibi imaging in head and neck cancer affected by MDR status, p53 expression or cell proliferation? *Nucl Med Biol* 1998; 25:593–541.
39. Kawai K, Fujibayashi Y, Saji H, et al. A strategy for the study of cerebral amino acid transport using iodine-123-labelled amino acid radiopharmaceutical: 3-iodo-alpha-methyl-L-tyrosine. *J Nucl Med* 1991; 32:819–824.
40. Langen KJ, Coenen HH, Roosen N, et al. SPECT studies of brain tumors with L-3-[^{123}I] iodo-alpha-methyl tyrosine: comparison with PET, ^{124}IMT and first clinical results. *J Nucl Med* 1990; 31:281–286.
41. Kuwert T, Morgenroth C, Woesler B, et al. Uptake of iodine-123-alpha-methyl tyrosine by gliomas and non-neoplastic brain lesions. *Eur J Nucl Med* 1996; 23:1345–1353.
42. Woesler B, Kuwert T, Morgenroth C, et al. Non-invasive grading of primary brain tumours: results of a comparative study between SPET with ^{123}I-alpha-methyl tyrosine and PET with ^{18}F-deoxyglucose. *Eur J Nucl Med* 1997; 24:428–434.
43. Weber W, Bartenstein P, Gross MW, et al. Fluorine-18-FDG PET and iodine-123-IMT SPECT in the evaluation of brain tumors. *J Nucl Med* 1997; 38:802–808.
44. Guth-Tougelidis B, Müller S, Mehdorn MM, Knust EJ, Dutschka K, Reiners C. DL-3-^{123}I-iodo-methyltyrosine uptake in brain tumor recurrences. *Nuklearmedizin* 1995; 34:71–75.
45. Ishii K, Ogawa T, Hatazawa J, Kanno I, Inugami A, Fujita H, Shimosegawa E, Murakami M, Okudera T, Uemura K. High L-methyl-[^{11}C]methionine uptake in brain abscess: a PET study. *J Comput Assist Tomogr* 1993; 17:660–661.
46. Tashima T, Morioka T, Nishio S, et al. Delayed cerebral radionecrosis with a high uptake of ^{11}C-methionine on PET and ^{201}Tl-chloride on SPECT. *Neuroradiology* 1998; 40:435–438.
47. Wunderlich G, Schmidt D, Langen KJ, et al. Evaluation of chemotherapy in gliomas by I-123-methyltyrosine SPECT: first results. *Eur J Nucl Med* 1995; 22:796.
48. Otto L, Dannenberg P, Feyer P, et al. Iodine-123-methyl-tyrosine uptake of brain tumors – influence of radiotherapy. *Eur J Nucl Med* 1995; 22:796.
49. Goldman S. Regional glucose metabolism and histopathology of gliomas. A study based on PET-guided stereotactic biopsy. *Cancer* 1996; 78:1098–1106.
50. Tatter SB, Wilson CB, Harsh GR. Neuroepithelial tumors of the adult brain. Neurological surgery, 4th edn, vol 4. Philadelphia: Saunders; 1996:2612–2684.
51. DiChiro G, Fulham MJ. Virchow's shackles: can PET-FDG challenge tumor histology? *AJNR* 1993; 14:524–527.